UNSTEADY EFFECTS OF A TRACTOR PROPELLER ON A LAMINAR WING: AN EXPERIMENTAL SETUP

D. P. Seyfert*, U. Deck*, J. Geiger[†]

* University of Stuttgart, Institute of Aerodynamics and Gas Dynamics, Wankelstr. 3, 70563 Stuttgart
† Student Assistent, University of Stuttgart

Abstract

Interaction effects between tractor propellers and wings have gained renewed attention in recent years due to the energetic advantage propeller-driven configurations offer compared to conventional jet engines in low to mid speed flight scenarios. While much of the existing research focuses on global effects, such as swirl recovery and vortex attenuation, previous publications suggest that viscous effects, particularly those concerning boundary layer development, can be equally important in optimizing the aerodynamic performance. Traditionally, it has been assumed that a propeller's turbulent wake causes the boundary layer of the adjacent wing to become fully turbulent. It has, however, been demonstrated, that laminar flow can persist in certain regions of the boundary layer, even in the vicinity of a propeller wake through a effect known as boundary layer relaxation. By this, the drag advantage offered by airfoils which are designed to maintain an extended area of laminar flow can be partially achieved for propeller-driven aircraft. In this paper, an experimental design is presents which aims to investigate the interaction between a propeller wake and a natural laminar flow (NLF) airfoil. First, the current state of research is laid-out to provide context for the integration of NLF wings and propeller-driven configurations. Based on these insights, specific requirements for the experimental setup are derived. Finally, measurement data for a reference configuration is provided, offering a comparative dataset for upcoming measurements.

Keywords Aerodynamics; Experiment; Boundary Layer; Propeller; Interaction

Symbols		
b	Number of Propeller Blades	-
c	Airfoil Chord Length	m
C_L	Drag Coefficient	-
J	Advance Ratio	-
C_L	Lift Coefficient	-
C_p	Pressure Coefficient	-
C_T	Thrust Coefficient	-
D	Propeller Disk Diameter	N
f_b	Blade Pass Frequency	$_{\mathrm{Hz}}$
f_{Tu}	Turbulence Frequency	m/s
k_{korr}	Correction Factor	-
n	Revolutions per Second	$_{ m Hz}$
N_{crit}	Critical N-Factor	-
r	Radial Position	m
R	Propeller Disc Radius	m
T	Propeller Thrust	N
Tu	Turbulence Intensity	-
${ar u}'$	Mean Velocity Perturbation in ${\bf x}$	m/s
U_{∞}	Free Dtream Velocity	m/s
ho	Air Density	$\rm kg/m^2$

NOMENCLATURE

Abbreviations

	AoA	Angle of Attack
-	BL	Boundary Layer
m	DFG	Deutsche Forschungs Gemeinschaft
-	LWT	Laminar Wind Tunnel
-	LST	Linear Stability Theory
_	NLF	Natural Laminar Flow
_	RANS	Reynolds Averaged Navier Stokes
N	Re	Reynolds (-number)
$_{\mathrm{Hz}}$	TS	Tollmien-Schlichting

1. INTRODUCTION

Laminar wings for moderate Reynolds (Re) numbers, where significant laminar flow can be achieved, offer a substantial drag advantage compared to configurations which use fully turbulent airfoils. They rely on specifically designed airfoils, known as Natural Laminar Flow (NLF) airfoils, to maintain an extended laminar run. The gained drag benefit directly translates into reduced fuel consumption, making NLF wings a possible solution for reducing emissions and the overall environmental impact of aviation. However, the application of NLF airfoils has been mostly limited to sailplanes or wind turbines, which exhibit Reynolds numbers and geometries which are greatly favourable for laminar boundary layers (BL). It could be shown that, while not to their full extend, laminarity can be partially maintained even in areas of strong

CC BY-NC 4.0 doi: 10.25967/630099

induced turbulence, such as the wake generated by a propeller in a tractor configuration [1], [2].

However, the influence of propeller wake on the laminar boundary layer, particularly under realistic flight conditions, remains insufficiently understood.

The DFG-funded collaborative research project "Synergies of Highly Integrated Transport Aircraft" (SynTrac) aims to explore synergistic effects at the overall aircraft level [3]. In this context, the feasibility of employing NLF wings in combination with distributed propulsion or traditional propeller-driven setups will be systematically investigated. Aircraft which use propellers as propulsor offer efficiency advantages over jet engines, especially at lower to moderate flight speeds, making them a compelling option for sustainable aviation.

Despite the individual benefits of NLF wings and propellers, there is limited knowledge on how NLF airfoils perform in the turbulent wake of a tractor propeller. This study addresses this gap by examining the boundary layer development of an NLF wing subjected to propeller wake interference. A novel experiment has been designed at the Laminar Wind Tunnel (LWT) at the University of Stuttgart to systematically study such an interaction scenario.

This paper serves as a foundation for future investigations by providing an overview of the experimental setup and initial reference measurements. First, the current state of research will be discussed before formulating requirements for an experiment to investigate the descriped scenario at conditions representative for aviation. At the end of this paper, first reference measurements will be presented and compared to standard numerical methods to establish a reliable baseline for future work.

2. STATE OF RESEARCH

The aerodynamic interaction between propellers and wings have been studied extensively on an experimental and numerical basis (e.g. [4] [5]). Early investigations date back to the 1920s [6], where studies explored the influence of vortical propeller wakes on the performance of wings and aircraft through in-flight and wind tunnel measurements [7]. Over the years, several systematic phenomena caused by the propeller wake on wing aerodynamics could be identified. In 1969, wind tunnel investigations on wingtipmounted propellers demonstrated that the induced drag produced by a wing could be reduced by counter rotating the propeller to the wingtip vortex [8]. An effect which is now knows as vortex attenuation. The study also highlighted up- and downwash effects, where the local angle of attack on the wing varies depending on whether it is exposed to the rising or falling side of the propeller. In the region affected by the rising blade, the flow's velocity vector tilts upward, resulting in locally reduced drag and increased lift, while the region in the vicinity of the falling propeller blade experiences the opposing effect.

In 1995 experiments employing integral balance measurements together with five-hole probe surveys were performed [9]. These provided detailed insights into the wake of an airfoil deformed by the influence of a propeller. The observed wake deformation was identified as an indicator for the propeller-altered lift distribution and thus the propellers influence on the wing's induced drag. Further experimental investigations and numerical simulations, including those by Stokkermanns [4], confirmed these findings. Stokkermanns investigated the flow field of five

different propeller-wing configurations. He employed measurements using a 6 component rotating shaft balance system, surface pressure tabs, stereo-PIV for flow field data, for integral force and for phase locked measurements. His findings could be reproduced through numerical simulation. In his research Stokkermanns, like the vast majority of the conducted experimental and numerical investigations, focus on global interaction effects, such as vortex attenuation, which affect the wing on an inviscid scale.

The propellers rotational wake greatly increases the flows unsteadiness which influences the flows turbulent intensity, at least on an averaged time interval. Accordingly, early experimental investigations conducted in 1920s and 1930s came to the conclusion, that the boundary layer exposed to a tractor propeller's slip stream becomes fully turbulent up to a point close to the wing's leading edge.

Young and Morris [10], through flight experiments, and Hood and Geydos [11], through wind tunnel studies, examined the impact of propeller wake on boundary layer behavior in 1939. Their employed method relied on the evaluation of the boundary layer thickness through velocity profiles using total pressure tubes. They identified the transition location where the boundary layer thickness exceeded theoretical values. Both studies concluded that the presence of the propeller wake caused the transition front to move close to the wing's leading edge, independent of the propeller cycle. Zalovik and Skoog [12], using highspeed in-flight measurements on a P-47 aircraft, observed that the propeller slipstream caused the transition front to move from 50% to around 25% of the chord length. This finding already suggested a less severe impact of the propeller on the boundary layer state than what Young and Hood had predicted.

In 1983, Holmes postulated the possibility of a cyclic state change in boundary layer behaviour [13]. From the data recorded through a boundary layer rake in a flight experiment, he compared time-averaged boundary layer velocity profiles inside and outside the slipstream. When comparing the velocity profiles in and outside of the propeller wake for clean and tripped wings, he observed that the shape of the boundary layer velocity profile inside the slipstream appeared "more turbulent" in nature, while still showing large deviations in to a actual turbulent boundary layer in the tripped configuration. He concluded that the early measurements conducted by Young and Morris likely reflected an averaged state of a boundary layer, experiencing cyclic disturbances from passing "turbulent packets," with the boundary layer in between remaining laminar.

In 1984, Holmes further stated that the benefits of natural laminar flow (NLF) airfoils could, at least partially, be maintained within the propeller slipstream, leading to a drag reduction compared to fully turbulent wings, even in multi-engine configurations with wing-mounted propellers [14]. This theory was later confirmed by Miley and Howard through both wind tunnel and flight experiments. In 1988, Miley examined the boundary layer behavior using hot wire probes for time-resolved measurements [1]. He investigated shape parameters for different regions of the boundary layer in the propeller wake and introduced the term "laminar revision" to emphasize the convective nature of the phenomenon, contrasting it with the well-known process of relaminarization .

A year later, Howard and Miley conducted a similar set of measurements in both wind tunnel and in-flight experiments [15]. In addition to Miley's findings, they discovered that the detected drag value in the propeller wake region

CC BY-NC 4.0

2

Author	Year	Chord Re-Number	Type	Wing BL	Flow Field	Pressure Tabs	$\mathrm{Tu}/\%$
Veldhuis [9]	1995	$0.82 \cdot 10^{6}$	phase locked	no	yes	yes	≈ 0.025
Stokkermanns [4]	2020	$\approx 0.74 \cdot 10^6$	phase locked	no	yes	yes	0.1 - 0.24
Miley [1]	1988	$0.6 \cdot 10^{6}$	time resolved	yes	no	no	in-flight
Howard [15]	1989	$0.6 - 1.2 \cdot 10^6$	time resolved	yes	no	no	0.3
Horstmann [2]	1994	$13 \cdot 10^{6}$	time resolved	no	no	yes	in-flight
Halstead [16]	1995	$1.5 - 5.3 \cdot 10^6$	phase locked	yes	no	no	5.5 - 16
Gostelow [17] [18]	1996	$0.117\cdot 10^6$	phase locked	yes	yes	no	-

TAB 1. Overview of the measurements conducted in a selection of the presented research. Where the Reynolds number was not explicitly provided, it was calculated using given geometric and flow data (marked by \approx). If environmental information were missing, ICAO standard values were assumed. For Halstead, only the first publication is referenced. It is important to note that Horstmann used hot film surface sensors but did not fully resolve the boundary layer. Most of Gostelow's measurements were performed on flat plates with Falkner-Skan boundary layers.

cycled between that of an undisturbed laminar state and a value lower than that of a fully turbulent wing .

In 1994, Horstmann et al. performed flight tests on a Dornier Do 228 aircraft, which was equipped with a laminar wing glove in the propeller wake area [2]. The aircraft was fitted with various sensors, including infrared cameras, hot film sensors, a wake rake, and pressure taps. Horstmann could recreate the findings of Holmes and measured time averaged pressure distributions in and outside of the propeller wake. He showed that a significant portion of the drag advantage offered by NLF airfoils in comparision to fully turbulent ones can be maintained, even if submerged inside the propeller slipstream .

A different research area where the cyclic transition of boundary layer due to periodic external disturbance is still of great interest is the field of turbomachinery. This is due to the long time reliance on empirical design parameters for blade design. A deeper understanding of the flow physics within periodic wake regions has been proposed as a means to enhance blade geometry development to improve the jet engines efficiency, stall margins, and pressure rise capabilities.

The basis for this is the work done by Schuhbauer and Klebanov in 1955 [19]. They investigated the boundary layer behaviour of a flat plate exposed to passing turbulent spots using hot wire anemometry. During their investigations they found that after the spots passage, the boundary layer would start to relax back to its laminar state. They named the area in the extent of the relaxation the calmed region and showed, that this region could have stabilizing effects on the trailing boundary layer, increasing the length of the laminar run. Findings which are similar to the much later experiments stated above.

Thus, after the work of Schuhbauer and Klebanov, a large quantity of studies have been carried out on the impact of turbulent spots on boundary layer development. These investigations include work on cascaded turbulence sources (e.g. [20], [21]) experiments under favourable, adverse or modeled pressure gradients (e.g. [22]), or full engine models (e.g. [23])

Two notable sources of research are the work of Halstead and Gostelow. In 1995, Halstead published four consecutive papers on the behaviour of turbulent spots and the calmed region based on experiments conducted in a research turbine [16]. Here, he investigated the boundary layer behaviour through surface hot-film and hot wire experiments where he identified different flow regions based on quasi shear stresses under the influence of changing Reynolds number, turbulence intensity and blade pass frequency.

At the same time, Gostelow studied the behaviour of the calmed region, first based on measurements on a flat plate and later on a research engine, using pressure tabs and hot wire probes [17] [18]. He found that, while the trailing edge velocity of the turbulent spot is highly affected by the present pressure gradient, the velocity of its leading edge stays relatively constant. Additionally, Gostelow was able to show strong relations between the BL behaviour on the investigated flat plates with artificial turbulence sources and its behaviour in an active turbine.

The presented literature review demonstrates that the extensive research conducted on propeller-wing interactions focuses almost exclusively on global interaction effects. Investigations on propeller-boundary layer interactions remain scarce. A comparison with findings from turbomachinery research reveals significant similarities in observed boundary layer behaviour. For instance, the phenomenon of "laminar revision" noted by [1] shows strong resemblance to boundary layer relaxation, including the calmed region. Table 1 gives an overview of the measurements conducted in some of the presented studies.

3. EXPERIMENTAL REQUIREMENTS

The objective for future studies is to conduct a detailed investigation into the influence of a periodic propeller wake on a laminar wings' boundary layer. Specifically, the research aims to characterize the distinct flow regions, including periodically laminar and turbulent boundary layers, as well as the effect of boundary layer relaxation and the calmed region. Therefore, the designed experiment has to have the ability to study key boundary layer properties and the propagation behavior of disturbances within named regions, all under conditions representative of real-world aviation. In the following chapter, general requirements for such investigations will be formulated.

Most literature focuses on on the global, inviscid scale rather than a detailed investigation of boundary layer effects.

Existing research focusing on wing boundary layers under aeronautical conditions dates mainly from the late 1980s to the mid 1990s. These studies provide first insights into the phenomenology of boundary layer relaxation inside the realm of aviation, but lack the in-depth analysis required to fully characterise boundary layer dynamics. Where boundary layer measurements have been made, they mostly consist of velocity profiles. For a better understanding it would be helpful to complement already existing insights by information on spectral amplification and dampening properties

CC BY-NC 4.0

3

of the boundary layer as well as its receptivity under the influence of the propeller wake.

Although more detailed and numerous analyses have been carried out in the field of turbomachinery, these studies usually focus on isolated or cascaded turbulent spots. However, the internal flow characteristics relevant for compressor or turbine stages in jet engines are dominated by turbulence levels and Reynolds numbers that differ by orders of magnitude from those encountered in external flow over wings. Hence, a direct translation of results from turbo machinery research to the field of wing aerodynamics might prove difficult.

In order to address the research objectives stated at the beginning of this chapter, several requirements can be formulated regarding the experimental investigations on the influence of a propeller wake on a wing boundary layer.

Representative Reynolds numbers: The Reynolds number at which the experiments are performed must be representative of those encountered in manned aviation, as the selected Re number strongly affects both transition and flow separation. By ensuring that the experiments are conducted at aviation-relevant Reynolds numbers of $\text{Re} \geq 10^6$, the results will be more applicable to real-world scenarios.

Representative turbulence intensity: Similar to the Reynolds number, turbulence intensity of the experiment must stay in a range which can be found at general and commercial aviation. The composition and the integral value of turbulence influence the boundary layer transition on both a quantitative and qualitative level. Previous research shows, that the turbulence intensity at typical cruise heights (above the athmospheric convective layer) of most commercial planes lies in the order of Tu=0.02% [24]. While there is no sharp separation between transition mechanism, a comparison and associated turbulence levels, it can be stated, that for flat plate investigations the main driver for laminar to turbulent transition for a $Tu\lesssim0.2\%$ are Tollmien-Schlichting (TS) waves [25].

Detailed Boundary Layer Measurements: The main focus of the conducted measurements will be to gain detailed insights into the boundary layer behaviour for the investigated interaction scenario. For this, measurement methods which are able to resolve both turbulent and laminar boundary layers are necessary. Measurement of boundary velocity profiles at multiple chord wise positions and their spectral analysis are essential to investigate the amplification or damping of specific frequency regions. These measurements are critical for understanding how the boundary layer evolves under the influence of the propeller wake, particularly during the complex process of transition. Naturally, a wing designed to allow for long laminar runs is necessary to aid an additional requirement for the planned measurements.

Highly resolved spatial measurements: The wake structure generated by a propeller is a highly complex, three dimensional phenomenon, which can be separated based on spanwise regions inside the propeller wake. If r is used to describe the radial position on the propeller disc with its origin at the center of the nacelle and R describes the propeller disk's radius, areas close to r/R=0 are mainly influenced by the nacelles wake and hub vortex whereas regions approaching r/R=1 will be strongly influenced by the propeller tip vortex. Areas in between are subject to up- and downwash effects as well as the viscouse blade wake, based on their spanwise position and the propellers sense of rotation.

Highly resolved temporal measurements: The blade passing frequency f_b , which is defined as

$$(1) f_b = n \cdot b$$

where n represents the propellers rotational frequency in Hz and b the number of blades, is the dominant frequency that introduces periodic disturbances into the flow field. However, for a comprehensive investigation of boundary layer dynamics, it is necessary to resolve frequencies which are significantly higher.

In order to assess the impact of the propeller on boundary layer transition, it is crucial to investigate how TS waves are either amplified or attenuated during their interaction with the propeller wake compared to the natural transition scenario. For Re-number of the LWT, the relevant TS waves are in the frequency range of approximately 500 to 6000 Hz in the context of the to be conducted experiments. To resolve these frequencies, a synchronized measurement system capable of a high temporal resolution of at least 12kHz per channel is necessary to ensure that the influence of the propeller wake on boundary layer stability and transition is accurately captured, according to Nyquist's Theorem.

Phase-Locked measurements: The interaction between propeller wake and wing is of periodic nature, defined through a constant cycle of bypass transition caused by passing wake sheets, relaxation of the wings boundary layer in the calmed region and by a conventional laminar boundary layer. In such a scenario, phase-locked measurements allow for the investigation of systematic boundary layer response across multiple wake passage cycles. This allows to investigate the different wake regions and boundary layer response in a systematic manner. Additionally, different measurement devices can be synchronized at f_b to create a composite picture of the interaction domain.

Measurements of unsteady surface pressure: In previous measurements, knowledge of unsteady or phase locked surface pressure coefficients (C_p) has proven a valuable asset to evaluate interaction effects on a global scale, such as the propellers influence on the wings lift distribution [4] or local velocity and pressure fluctuations. With a high enough frequency resolution, phase locked C_p distributions allow for insights on the influence of the propeller wake on laminar separation bubbles or phenomena such as dynamic reattachment which may be triggered by the upwash effects on the rising propeller blade side. Further, high frequency surface pressure data can be employed to identify the onset of boundary layer transition, offering additional insight into the interaction between the propeller wake and the wing surface.

Integral and flow field measurements: To obtain a complete picture of the investigated setup, time averaged load measurements across the full model are beneficial. These measurements will complement the local and phase-locked data by providing an overall understanding of the interaction between the propeller wake and the wing, enabling more comprehensive conclusions to be drawn from the experimental data.

4. EXPERIMENTAL SETUP

4

The following section gives an overview of the designed wind tunnel experiment. Based on the requirements formulated above, the experiment aims to provide a setup ca-

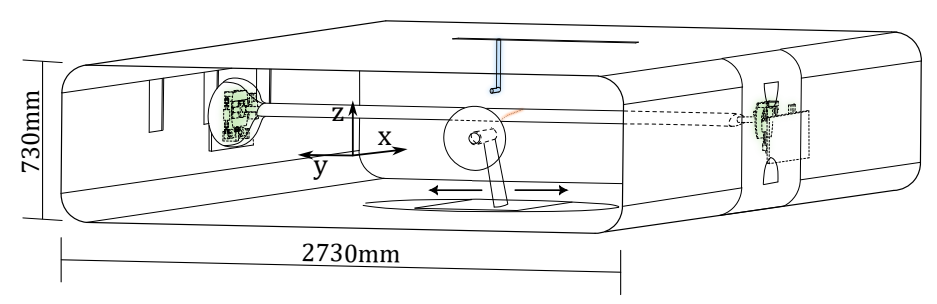


FIG 1. Sketch of the experimental setup. Highlighted in green are the custom built wind tunnel scales, highlighted in orange the Kulite pressure transducers and highlighted in blue the Vectoflow five hole probe. For a better overview, the aerodynamic housing on the right balance system is not displayed.

pable of investigating the interactions between the tractor propeller and a laminar wing under conditions representative for aviation.

The overview is divided into several parts. First, the wind tunnel for the experiments is introduced to gain a deeper understanding of the capabilities of the facility and its suitability for this study.

Next, the design of the laminar wing model and the propeller system, including the traversing system, is described. These elements form the core of the experimental setup and are essential to replicate realistic aerodynamic conditions. Finally, the measurement equipment is presented, detailing the custom-built wind tunnel balance and other measurement systems used to capture integral quantities, boundary layer dynamics and flow field data with high temporal and spatial resolution.

4.1. The Laminar Wind Tunnel

The Laminar Wind Tunnel (LWT) at the Institute of Aerodynamics and Gasdynamics is a open-return style wind tunnel with a closed test section of $0.73 \mathrm{m} \times 2.73 \mathrm{m}$ and $3.15 \mathrm{m}$ length.

Its inlet features an effective contraction ratio of 20:1 and flow conditioning in form of two screens, leading to an unseparated, isotropic turbulence intensity

$$(2) Tu = \sqrt{\bar{u}^{\prime 2}}/U_{\infty}$$

of $Tu \leq 0.02\%$ for $U_{\infty} = 40 \mathrm{m/s}$ over a frequency range of $10 \mathrm{Hz} \leq f_{Tu} \leq 5000 \mathrm{Hz}$ Additionally, the test section is enclosed by an airtight measurement chamber. During measurements the pressure inside the measurement chamber is adjusted to a value below the minimum static pressure inside the test section. This prevents air leakage into the test section.

For standard polar measurements, the wing model is installed vertically into the test section and integral lift and drag measurements are conducted through minimally intrusive measurement methods. Lift is measured through pressure projection and integration on the tunnel walls. Drag is measured using a traversable wake rake system with automatic alignment, located at approximately $1.5 \cdot c$ behind a wind tunnel model with $c=350 \mathrm{mm}$. Standard wind tunnel corrections are applied to the recorded lift and drag coefficients, standard wind tunnel corrections are applied [26] [27].

4.2. Wing and Propeller Models

The employed NLF airfoil DP-FR-1924-MODLWT in this experimental setup was specifically designed for this measurement campaign. The wing features a chord length of 350mm, chosen to achieve a realistic c/D ratio. The airfoil

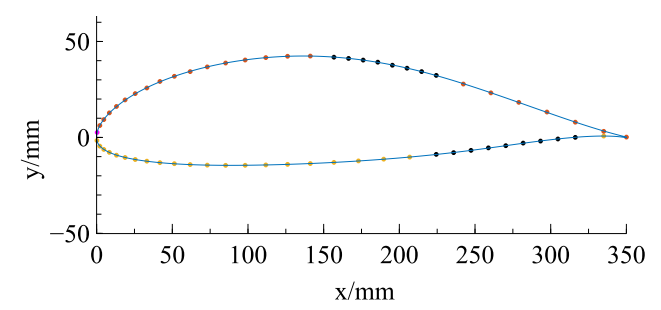


FIG 2. DP-FR-1924-MODLWT airfoil, based on the design and with courtesy from. The chordwise positions of pressure tabs are displayed as dots. For the 2.3m model, only the positions at the suction side will be equipped with Kulite sensors.

was designed to operate at a Reynolds number of 1.5×10^6 . For the experiments, two different wing configurations will be employed. The first wing has a span of 0.73m for standard vertical installation inside the LWT. This model, refered to as the reference model, will be employed to generate reference aerodynamic data. The second wing configuration has a total span of 2.3m and will be used to investigate the propeller-wing interaction. An overview of the horizontal measurement setup can be seen in Figure 1. The built-in instrumentation, which will be discussed in a later section, allows for high-resolution measurement of flow characteristics and boundary layer dynamics. Figure 2 shows the designed airfoil. Normalized coordinates of the airfoil can be accessed in [28].

The propeller used in the experiment is a two-bladed, fixed-pitch model with a disk diameter of 0.3m. The propeller is driven by a 4.5 kW electric engine, housed within a nacelle. The nacelle is mounted to a traversing system outside of the test section, allowing for a precise and repeatable change in the propellers spanwise position relative to the wing. With this setup, the propeller can be traversed in a range of ± 0.25 m in spanwise direction, related to the center of the test section.

To generate a realistic wake field the two defining dimensionless quantities are the propellers thrust coefficient C_T and its advance ratio J

(3)
$$C_T = \frac{T}{\rho n^2 D^4}$$

$$(4) J = \frac{U_{\infty}}{nD}$$

where T is the thrust produced by the propeller. The propeller used for the experiment was designed at a operation point of $C_T = 0.12$ and J = 2.24. These values can be

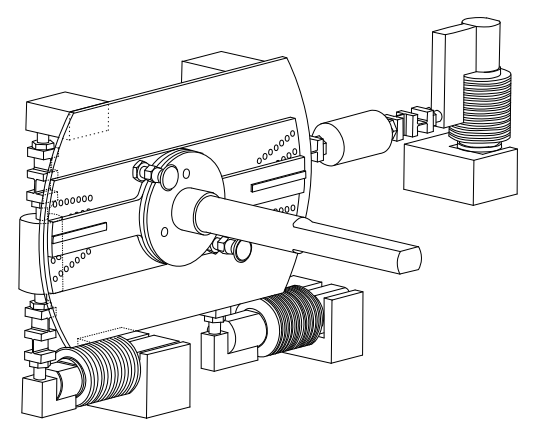


FIG 3. Sketch of one LWT Balance unit to measure time averaged lift and drag. The each load cell is connected by two flexures to the attachment unit.

seen as representative for propellers with low disk loading as employed in a distributed propulsion scenario [29]. The selected realistic propeller operation point combined with the low blade number is expected to produce a wake with extended spacing between passing turbulent wake sheets. This, in conjunction with the extended laminar run of the NLF airfoil, theoretically permits long stretches of laminar flow between the periodic passages of turbulent wake sheets. Such conditions provide a potentially excel-

lent environment for the investigation of boundary layer

4.3. Instrumentation

relaxation and the calmed region.

This chapter introduces instrumentation. Figure 1 illustrates the unconventional configuration used for the interaction scenario, highlighting key components and a number of sensors used in the experiment. The propeller traversing system, indicated by the arrows next to the propeller pylon, enables the acquisition of high-resolution spatial data across different span positions. This system eliminates the need for a large number of sensors or manual repositioning, significantly improving measurement efficiency. By use of the traversing system, a single sensor at a given chord position is capable to record data at arbitraty spanwise positions in the range of $r/R \in [-1.10, 1.10]$. This creates a fine grid for the spatial resolution of the experiment.

The following section provides an overview of the various measurement systems employed in the experimental setup. These include the wind tunnel balance system, the surface pressure measurement setup, the boundary layer probe, and a five-hole probe.

In order to measure the global lift, drag and pitching moment acting on the wing, a custom three-component balance system was designed for use in the experiment. The balance system is organized in two symmetrical balance units (see Figure 3). Each unit consists of one ME-Meßsysteme KD120 and a HBM Z6 load cell with maximum load capacities of 2kN and 1kN for lift measurements as well as a single KD120 load cell 200N for drag measurements. These units are mounted on the walls of the test section and are directly connected to the wing. To achieve the decoupling of lift and drag forces, the system utilizes specially designed flexures. These flexures are characterized by very low area moments of inertia in two spatial directions, while maintaining high stiffness in the direction of measurement. This design ensures that

the flexures minimize cross-talk between lift and drag measurements.

During installation, the load cells are carefully aligned to the wind tunnel's coordinate system to ensure precise measurements of both drag and lift forces. The balance system is precision-manufactured using CNC technology and mechanical steel to ensure a high component accuracy and stiffness. The alignment of the components relative to each other is maintained through dowel pins. Any potential alignment errors can be identified by comparing results from measurements taken without the propeller, as well as from reference configuration tests.

The balance system incorporates an adjustment mechanism that enables the precise setting of the wing's angle of attack (AoA). This system allows for a stepwise and repeatable adjustments of the AoA in 0.1° increments. To prevent dynamic instabilities during operation and avoid structural stress, one of the balance units is connected to the wind tunnel wall in the spanwise direction using a flexible rod. This rod serves a similar function as the flexures, characterized through high stiffness in wall normal direction while remaining flexible in directions perpendicular to the wind tunnel wall.

Both balance units are covered by streamlined, aerodynamic housings. These aprevent the influence of parasitic aerodynamic forces on the balance system, ensuring that the measurements are solely indicative of the forces generated by the wing and propeller during testing.

A total of 32 Kulite XCS-SL-062 miniature pressure transducers are installed flush with the surface on the suction side of the of the interaction wind tunnel model (see figure 1, highlighted in red). These sensors are aligned at an angle of 15° along the chord direction, relative to the x-z plane of the wind tunnel. The transducer density is higher in regions where a steep pressure gradient is to be expected. Their exact location is displayed as dots on the suction surface of Figure 2. The transducers will be used to gather both steady and unsteady surface pressure data, which will provide critical information on transition monitoring, propeller induced alteration of the lift and pressure coefficient and pressure drag components in the propeller's slipstream. Additionally, these sensors enable complementary investigations into the effect of the propeller on laminar separation bubbles that form on the airfoil's surface. The surface-flush installation of the transducers eliminates the need for pressure tubing, which significantly enhances the dynamic response of the sensors. This configuration minimizes phase lag as well as dampening and prevents standing wave issues, ensuring that the spectral flow char-

The angle under which the sensors are installed aims towards minimizing the influence of upstream on downstream sensors. Imperfections on the models surface due to sensor installation could destabilize the wings boundary layer, causing turbulent wedges to form. The 15° installation angle prevents downstream sensors to be positioned inside a possible upstream turbulent wedge.

acteristics are recorded in good quality.

Detailed investigations of the propeller - BL interaction will be conducted using constant temperature hot-wire anemometry. A tungsten hot wire, measuring $2.5\mu \rm m$ in diameter and 1.2mm in length, is mounted to a mechanism referred to as the Boundary Layer Probe [25]. This system enables precise and repeatable positioning of the probe, with a resolution of $5\mu \rm m$ in wall-normal direction.

Initial vertical positioning of the probe is achieved by establishing electrical contact between the probe and a con-

CC BY-NC 4.0

6

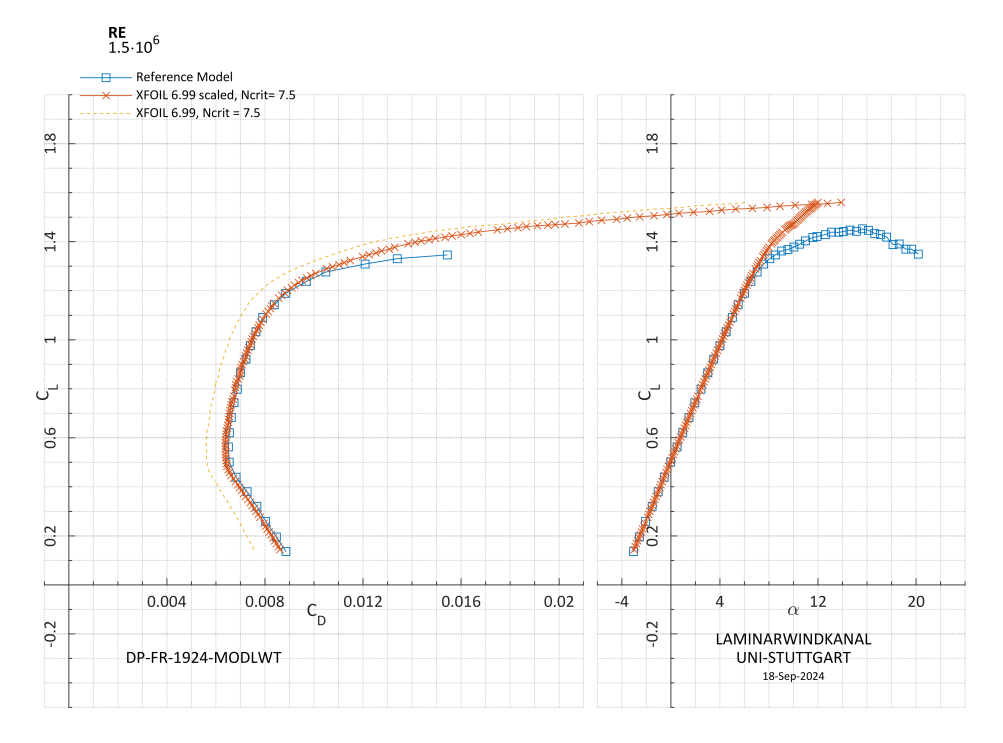


FIG 4. Measured reference data (blue) and a XFOIL calculation without (yellow) and with applied correction factor (orange). The XFOIL data was calculated based on $N_{crit} = 7.5$. A correction factor of $C_D/C_{D,Foil} = 1.14$ has been applied to the calculated C_D . For measurements above a $C_L = 1.35$, no C_D data is available, as the wake rake was removed from the flow to prevent possible damage.

ductive graphite layer on the model surface. Once the electrical contact is established, the probe is carefully moved in the z-direction until the electrical contact lost. This procedure ensures high repeatability in probe positioning while minimizing errors caused by probe bending or mechanical backlash.

To further reduce mechanical vibrations affecting the probe, a support strut is placed on the model surface 100mm downstream. Scruton spirals are attached to vertical cylindrical structures of the BL probe in order to avoid vortex shedding.

Flow field measurements in the wake region will be performed by a five-hole probe. This approach allows for a direct comparison between the flow field of the isolated propeller and the interaction case, providing information on wake structure and its deformation. Additionally, the five-hole probe will enable the determination of profile drag through wake integration, as described in [9]. This drag data can be used to calibrate the balance system using measurements from the reference configuration.

The five-hole probe selected for this task is a Vectoflow FRAP-Pro, which will be mounted on the wind tunnel traversing system 0.5m behind the wing's trailing edge. The probe will traverse a plane perpendicular to the main flow direction, allowing for highly resolved wake field measurements. The probe features a 3mm conical head with five pressure orifices, each 0.6mm in diameter. The tubing length has been adjusted to shift the probes' resonance frequency of away from f_b . Through careful frequency calibration and the use of the short tubing, the probe will be capable of measuring unsteady flow field data up to frequencies in the lower kHz range in both amplitude and direction.

Although not directly linked to boundary layer quantities in the interaction scenario, the five-hole probe will contribute to a complete picture of the aerodynamic setup by providing detailed insights into flow field data.

5. REFERENCE MEASUREMENTS

In the following chapter, the measurement results for the reference configuration are presented. To ensure accuracy and reliability, the experimental data is cross-validated against computational results from CFD simulations conducted with ANSYS Fluent 2022R2 and calculations performed using XFOIL (6.99). The investigated wing was manufactured in-house using a negative mold process to ensure high precision and measures 0.73m in span and 0.35m in chord. The presented results were obtained through the standard lift and wake integration measurement systems of the LWT.

Figure 4 shows the experimental results as well as a numerical comparison made with XFOIL6.99 [30]. The experimentally gathered results are displayed in blue while the calculated XFOIL values are shown in yellow. Due to XFOIL's tendency to slightly underpredict drag values [31], a global correction factor of $k_{corr} = 1.14$ was applied to XFOIL's' (C_D) values. The correction was implemented as follows:

$$\frac{C_{D}}{C_{D,Foil}} = 1.14$$

where $C_{D,Foil}$ represents the raw XFOIL output data. In both data sets a very pronounced laminar bucket with an extend of $\Delta C_L = 0.74$ is visible, stretching from $\alpha = 0$ ° to $\alpha = 6.5$ °. For the measurements, drag coefficient data is only available for values of $C_L \leq 1.35$, as measurements at higher values risk damaging the wake rake in regions of turbulent separation and compromise the measurement method. Thus, only C_L and α data is available in this

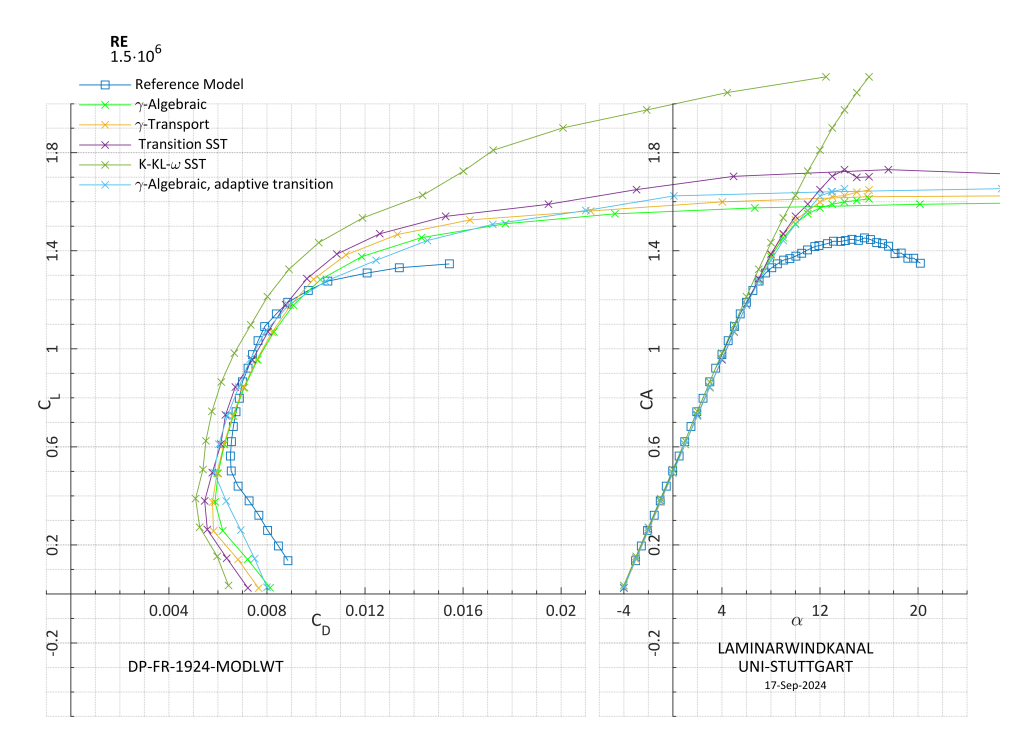


FIG 5. Measured reference data (blue) and polars generated with ANSYS Fluent 2022R2 RANS simulations.

region. The results, depicted in the blue, show the airfoil's stall behavior. The characterization of the airfoil indicates a minimum drag of $C_{Dmin}=0.0065$ with a corresponding lift coefficient of $C_L=0.56$ at the lower end of the laminar bucket. The measured maximum maximum lift coefficient is $(C_{L,max}=1.45)$ recorded at an angle of attack of $\alpha=15.6^{\circ}$.

The lower end of the laminar bucket is highly sensitive to changes in the laminar run. Therefore, to gain referential data, N_{crit} of the envelope method was specifically selected to minimize the prediction error at the lower corner of the laminar bucket and rounded to 0.5 accuracy.

The measured transition locations were detected using an stethoscope. The onset of transition is identified by a sharp increase in acoustic amplitude, which corresponds closely to the point where local skin friction begins to rise. This makes the acoustic detection method highly comparable to transition location measurements that rely on surface oil-film techniques.

Figure 6 displays both the measured and computed transition locations obtained from XFOIL. Within the laminar bucket, transition on the suction side of the airfoil occurs between $x_{TR}/c \in [0.55, 0.65]$ on the wings suction side and between $x_{TR}/c \in [0.70, 0.85]$ on its pressure side. The experimental values and XFOIL predictions generally align well, with a slight under prediction on the side of the calculations. The deviation between the measured and calculated value starts to increase near the stall region of the airfoil. This is also in good agreement with the deviations shown in Figure 4.

Additional Reynolds-Averaged Navier-Stokes (RANS) simulations were carried out on the reference model to further validate the experimental measurements. These simulations were carried using a selection of standard correlation-based transition models in combination with the well-known $k\omega$ -SST turbulence model [32].

The simulations were performed using ANSYS Fluent, employing an tow dimensional unstructured mesh that con-

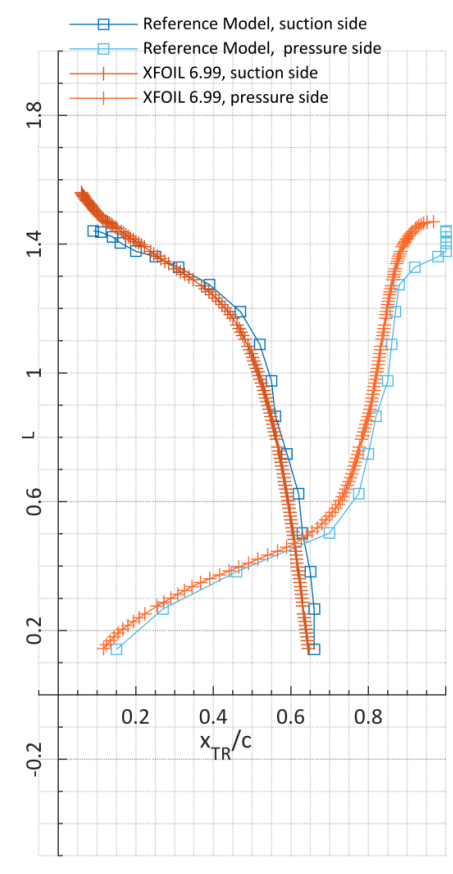


FIG 6. Measured and predicted transition locations for the Reference Model. Measured values are recorded in steps of $\Delta \alpha = 1$ ° and displayed in blue. XFOIL computed transition locations are displayed in orange.

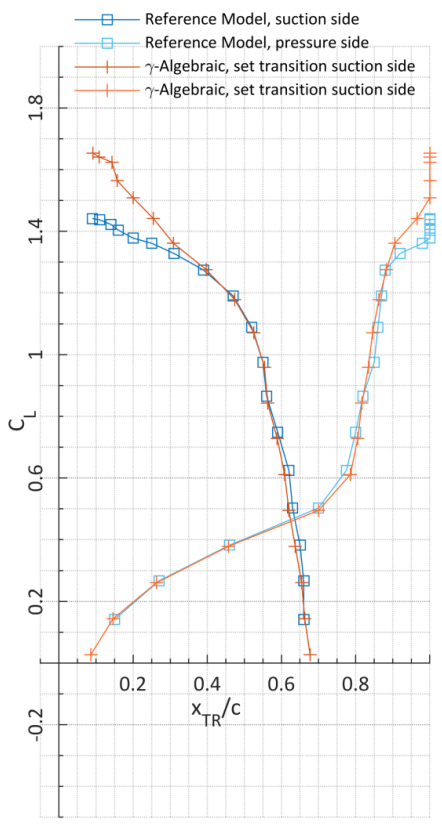


FIG 7. Measured and predicted transition locations for the Reference Model. Measured values are recorded in steps of $\Delta \alpha = 1$ ° and displayed in blue. Set transition locations for ANSYS are displayed in orange.

sisted of a total of 55681 cells, mainly quad elements. The

mesh design included a far-field cell size of 0.4m, the cell height of the first cell in the boundary layer is $5.5 \cdot 10^{-6}$ m, ensuring a y+ value below y+=1 for all investigated flow situations. The boundary layer mesh is extruded from the surface to gain a structured cell arrangement in the boundary layer regime. The transition models γ -Algebraic, γ -Transport, γ -Re- Θ (named "Transition SST" in Fluent), and K-KL- ω models were applied using default parameters. A separate simulation was conducted using the γ -Algebraic model, where the transition location was manually set to match the experimental transition data from Figure 7. Figure 5 provides an overview of the results. Overall, the computational results showed the expected agreement with the experimental data. In the region of the laminar bucket, except for the K-KL- ω model, the drag coefficients agree well with the measured values. The lift coefficient at the stall angle of attack is over predicted by all models, similar to the XFOIL results. In the region of the lower corner of the laminar bucket all models predict too optimistic transition s locations, resulting in too low drag coefficients. The custom calibrated γ -Algebraic model demonstrated the best agreement with the measured polar data, particularly at the lower end of the laminar bucket. Deviations in transition location for CL values above 1.2 could

the geometric angle of attack. The data of the measured polars and transition positions can be referenced at [33]

be attributed to discrepancies in the C_L α curve, as the

transition location was set based on C_L values rather than

6. CONCLUSION

The presented paper outlines the experimental setup designed to investigate propeller - boundary layer interaction in a scenario representative for aviation.

First, a overview of existing research was given which was then used to formulate experimental requirements necessary to gain in depth insights into boundary layer phenomena which are representative for propeller driven aircraft. These formulations were then used to design an experiment at the Laminar Wind Tunnel at the Institute of Aerodynamics and Gas Dynamics of the University of Stuttart. This experimental setup consists of a horizontal wing with a traversable propeller in front of it. The traversing system combined with phase locked measurements allow for a high spatial resolution of the measured quantities. The introduced measurement equiptment consists of kulite sensors, constant temperature anemometry, a custom designed balance system as well as a five hole pressure probe. Finally, this paper presents first results gathered through reference measurements. The measurements were cross validated through several state of the art numerical methods. The best correlation between the experimental measurements and computational predictions was achieved using the calibrated envelope method in XFOIL, with the expected deviations in the stall region of the airfoil. Similarly, the results from the RANS simulations fell within the expected margins of error, consistent with the known limitations of these methods. Overall, the experimental and computational results are in good agreement. Crucially, no evidence of measurement error was found throughout the study. In conclusion, the presented investigation provides a solid foundation for the further experimental exploration of natural laminar flow airfoils in interaction scenarios with tractor propellers. Thanks to the DLR Insitute of Aerodynamics and FLow Technology and the Institute of Fluid Mechanics of the TU Braunschweig for providing the baseline of the airfoil, from which the DP-FR-1924-MODLWT is derived from.

Funded by the Deutsche Forschungsgemeinschaft (DFG, German Research Foundation) – Project ID 498601949 – TRR 364

Contact address:

dominic.seyfert@iag.uni-stuttgart.de

References

- Stan J. Miley, Richard M. Howard, and Bruce J. Holmes. Wing laminar boundary layer in the presence of a propeller slipstream. Journal of Aircraft, 25(7):606-611, 1988. DOI: 10.2514/3.45630.
- [2] K-H Horstmann, R Mueller, C-H Rohardt, A Quast, H Echtle, W Wohlrath, P Dick, D Welte, and HW Stock. Design and flight test evaluation of a laminar wing glove on a commuter aircraft. ICAS, 1994.
- [3] Deutsche Forschungs Gemeinschaft. TRR 364: Synergien von hochintegrierten Transportflugzeugen SynTrac. https://gepris.dfg.de/gepris/projekt/4 98601949, 2023. [Accessed 18-09-2024].
- [4] TCA Stokkermans. Aerodynamics of propellers in interaction dominated flowfields: An application to novel aerospace vehicles. 2020.

- [5] Tomas Sinnige, Reynard De Vries, Biagio Della Corte, Francesco Avallone, Daniele Ragni, Georg Eitelberg, and Leo LM Veldhuis. Unsteady pylon loading caused by propeller-slipstream impingement for tip-mounted propellers. Journal of Aircraft, 55(4):1605–1618, 2018.
- [6] Ludwig Prandtl. Mutual influence of wings and propeller. Technical report, 1921.
- [7] James Sargent Russell and Howard Monroe McCoy. Propeller characteristics and slipstream effects on a high wing monoplane from wind tunnel tests. PhD thesis, California Institute of Technology, 1935.
- [8] MELVIN H. SNYDER and GLEN W. ZUMWALT. Effects of wingtip-mounted propellers on wing lift and induced drag. Journal of Aircraft, 6(5):392–397, 1969.
- [9] L Veldhuis and D Rentema. Quantitative wake surveys behind a tractor propeller-wing configuration. DOI: 10.2514/6.1995-3908.
- [10] Alec David Young and DE Morris. Note on flight tests on the effect of slipstream on boundary layer flow. HM Stationery Office, 1939.
- [11] Manley J Hood and M Edward Gaydos. Effects of Propellers and of Vibration on the Extent of Laminar Flow on the NACA 27-212 Airfoil. NACA, 1939.
- [12] John A. Zalovik and Richard B Skoog. Flight investigation of boundary-layer transition and profile drag of an experimental low-drag wing installed on a fighter-type airplane. Technical report, 1945.
- [13] BJ Holmes and CJ Obara. Observations and implications of natural laminar flow on practical airplane surfaces. Journal of Aircraft, 20(12):993–1006, 1983.
- [14] Bruce J Holmes, Clifford J Obara, and Long P Yip. Natural laminar flow experiments on modem airplane surfaces. NASA Tech. Pap, 2256, 1984.
- [15] Richard M Howard and Stan J Miley. Time-dependent boundary-layer response in a propeller slipstream. Journal of aircraft, 26(9):863–869, 1989.
- [16] David E Halstead, David C Wisler, Theodore H Okiishi, Gregory J Walker, Howard P Hodson, and Hyoun-Woo Shin. Boundary layer development in axial compressors and turbines: Part 1 of 4 Composite picture, volume 78781. American Society of Mechanical Engineers, 1995.
- [17] J. P. Gostelow, N. Melwani, and G. J. Walker. Effects of Streamwise Pressure Gradient on Turbulent Spot Development. Journal of Turbomachinery, 118(4):737–743, 10 1996. ISSN: 0889-504X. DOI: 10.1115/1.2840929.
- [18] J. P. Gostelow, G. J. Walker, W. J. Solomon, G. Hong, and N. Melwani. Investigation of the Calmed Region Behind a Turbulent Spot. Journal of Turbomachinery, 119(4):802–809, 10 1997. ISSN: 0889-504X. DOI: 10.1115/1.2841191.
- [19] Galen B Schubauer and Philip S Klebanoff. Contributions on the mechanics of boundary-layer transition. Technical report, NASA, 1956.

- [20] HP Hodson. An inviscid blade-to-blade prediction of a wake-generated unsteady flow. 1985.
- [21] W-P Jeon, T-C Park, and S-H Kang. Experimental study of boundary-layer transition on an airfoil induced by periodically passing wake. Experiments in Fluids, 32(2):229–241, 2002.
- [22] Response of a Laminar Separation Bubble to an Impinging Wake, volume Volume 6: Turbo Expo 2003, Parts A and B of Turbo Expo: Power for Land, Sea, and Air, 06 2003. DOI: 10.1115/GT2003-38972.
- [23] HP Hodson, I Huntsman, and AB Steele. An investigation of boundary layer development in a multistage lp turbine. 1994.
- [24] LJ Otten, AL Pavel, WC Rose, and WE Finley. Atmospheric turbulence measurements from a subsonic aircraft. AIAA Journal, 20(5):610–611, 1982.
- [25] Jonas Romblad. Experiments on the laminar to turbulent transition under unsteady inflow conditions. 2023.
- [26] D Althaus. Measurement of lift and drag in the laminar wind tunnel. University of Stuttgart Report, 2003.
- [27] D Althaus. Tunnel-wall corrections at the laminar wind tunnel. Institute report, IAG, http://www.iag. uni-stuttgart. de/laminarwindkanal, 2003.
- [28] Ulrich Deck and Dominic Seyfert. DP-FR-1924-MODLTW airfoil coordinates, 2024. DOI: 10.18419/darus-4490.
- [29] Tomas Sinnige. Aerodynamic and aeroacoustic interaction effects for tip-mounted propellers: an experimental study. 2018.
- [30] Mark Drela and Michael B Giles. Viscous-inviscid analysis of transonic and low reynolds number airfoils. AIAA journal, 25(10):1347–1355, 1987.
- [31] W Timmer. An overview of naca 6-digit airfoil series characteristics with reference to airfoils for large wind turbine blades. In 47th AIAA aerospace sciences meeting including the new horizons forum and aerospace exposition, page 268, 2009.
- [32] Florian R Menter. Two-equation eddy-viscosity turbulence models for engineering applications. AIAA journal, 32(8):1598–1605, 1994.
- [33] Dominic Seyfert. DP-FR-1924-MODLTW Polar Data Re15E5, 2024. DOI: 10.18419/darus-4491.